Adenovirus-mediated expression of SIK1 improves hepatic glucose and lipid metabolism in type 2 diabetes mellitus rats

DaoFei Song[1], Lei Yin[1], Chang Wang[1], XiuYingWen[2*]

1.Department of Endocrinology, Liyuan Hospital, Tongji Medical College, Huazhong University of Science and Technology, Wuhan, P.R. China

2. Department of Traditional Chinese Medicine and Endocrinology, Liyuan Hospital, Tongji Medical College, Huazhong University of Science and Technology, Wuhan, PR China

*Correspondence author

E-mail: wenxyoung@hust.edu.cn(XYW)

Abstract

AIM: In this study, we investigated the role and mechanism of Salt-induced kinase 1 (SIK1) in regulation of hepatic glucose and lipid metabolism in a high-fat food (HFD) and streptozocin (STZ)-induced type 2 diabetes mellitus (T2DM) rat model.

Methods: A diabetic rat model treated with HFD plus low-dose STZ was developed and was transduced to induce a high expression of SIK1 in vivo via a tail-vein injection of a recombinant adenoviral vector. The effects on hepatic glucogenetic and lipogenic gene expression, systemic metabolism and pathological changes were then determined.

Results: In T2DM rats, SIK1 expression was reduced in the liver. Overexpression of SIK1 improved hyperglycaemia, hyperlipidaemia and fatty liver, reduced the expression of cAMP-response element binding protein (CREB)-regulated transcription co-activator 2 (CRTC2), phosphoenolpyruvate carboxykinase (PEPCK), glucose-6-phosphatase (G6Pase), pS577 SIK1, sterol regulatory element binding-protein-1c (SREBP-1c) and its target genes, including acetyl-CoA carboxylase (ACC) and fatty acid synthase (FAS), and increased the expression of SIK1, pT182 SIK1 and pS171 CRTC2 in diabetic rat livers with the suppression of gluconeogenesis and lipid deposition.

Conclusion: SIK1 plays a crucial role in the regulation of glucose and lipid metabolism in the livers of HFD/STZ-induced T2DM rats, where it suppresses hepatic gluconeogenesis and lipogenesis by regulating the SIK1/CRTC2 and SIK1/SREBP-1c signalling pathways. Strategies to activate SIK1 kinase in liver would likely have

beneficial effects in patients with T2DM and nonalcoholic fatty liver disease (NAFLD).

Keywords: adenovirus; Salt-induced kinase 1; gluconeogenesis; lipogenesis; type 2 diabetes mellitus; diabetic rats

Introduction

T2DM is characterized by hyperglycemia and insulin resistance (IR) and is the foremost type of diabetes around the world [1]. Diabetes complications such as hyperlipidemia and NAFLD account for an increasing proportion of annual health care costs. Tight glucose control has been associated with a reduced incidence of diabetes complications, underscoring efforts to characterize regulators that function importantly in the pathogenesis of T2DM [2].

SIK1, a serine/threonine protein kinase, belongs to the AMP-activated protein kinase (AMPK) [3]. As an energy sensor, AMPK markedly inhibits hepatic glucogenesis and lipogenesis by transcriptional control [4, 5]. In addition, Liver kinase B 1 (LKB1), a major upstream kinase of AMPK, phosphorylates SIK1 at Thr182 in the activation loop (A-loop) of the kinase domain, which is essential for switching on the SIK1 kinase activity, thus resulting in the increase of the kinase activity of SIK1 [6, 7]. Treatment with adrenocorticotropic hormone (ACTH) and the subsequent phosphorylation of the regulatory domain at Ser-577 by protein kinase A (PKA) makes SIK1 translocate to the cytoplasm and lose its repressive properties[3, 8]. Knockdown of SIK1 in mice promoted both fasting hyperglycaemia and gluconeogenic gene expression. Conversely, mice treated with adenovirus-expressed

SIK1 (Ad-SIK1) exhibited fasting hypoglycaemia and reduce gluconeogenic gene expression [9]. Ad-SIK1 was also effective in reducing blood glucose levels in fasted db/db diabetic mice [9]. These observations demonstrate a key role of SIK1 on glucose metabolism in vivo.

The liver is the major organ responsible for glucose production. Hepatic glucose production mainly comes from gluconeogenesis and is critical for maintaining normoglycemia in the fasting state [10]. The cAMP response element binding protein (CREB) and its co-activator, CRTC2, play crucial roles in signal-dependent transcriptional regulation of hepatic gluconeogenesis. CREB transcriptional activity is required for fasting gluconeogenesis [11]. CRTC2 is a key regulator of fasting glucose metabolism that acts through the CREB to modulate glucose output. Phosphorylation of CRTC2 at Ser171 by AMPK results in the inhibition of the nuclear translocation of CRTC2; subsequently, the cytoplasmic localization of CRTC2 prevents its combination with CREB elements [9, 12]. Thus, gluconeogenesis is restrained. Conversely, sequestered in the cytoplasm under feeding conditions, CRTC2 is dephosphorylated and transported to the nucleus where it enhances CREB-dependent transcription in response to fasting stimuli [9]. CRTC2 has been recently found to be a substrate of SIK1 in vivo [9, 12]. SIK1 had been previously identified as a modulator of CREB-dependent transcription in adrenocortical carcinoma cells [13]. Moreover, CREB was found to occupy the SIK1 promoter in chromatin immunoprecipitation assays of primary rat hepatocytes; CRTC2 was recruited to this promoter in response to forskolin treatment [9]. The mRNA levels of CRTC2, PEPCK and G6Pase in

SIK1-deficient primary rat hepatocytes were increased, while SIK1 overexpression suppressed the CRTC2 activity [9]. A recent report has shown that the selective salt-induced kinase (SIK) inhibitor HG-9-91-01 promotes dephosphorylation of CRTC2, resulting in enhanced gluconeogenic gene expression and glucose production in hepatocytes, but this effect is abolished when an HG-9-91-01-insensitive mutant SIK is introduced [14]. Interestingly, in primary rat hepatocytes, SIK1 phosphorylated CRTC2 at Ser 171 and in turn promoted its export to the cytoplasm, thereby inhibiting the expression of downstream gluconeogenic genes such as PEPCK and G6Pase [9], suggesting that regulation of CRTC2 activity by SIK1 may be crucial for inhibiting excessive hepatic glucose output. Therefore, the SIK1/CRTC2 signalling pathway will probably represent a novel strategy for suppressing hepatic gluconeogenesis and ameliorating hyperglycaemia. Although SIK1 is implicated in regulation of CRTC2 and hepatic glucose output, the glycometabolism of the kinase remains uncharacterized in the HFD/STZ-induced T2DM rat model.

In addition, the liver is also one of the major organs regulating lipid metabolism [15]. Hepatic lipogenesis contributes to accumulation of fat in the liver [16]. SREBP-1c acts as a master transcriptional regulator for the hepatic lipogenesis by activating its target genes, such as FAS and ACC. Moreover, SREBP-1c is shown to be a direct substrate for SIK1 in vitro [17]. SIK1 blocks lipogenesis by direct phosphorylation of SREBP-1c on multiple serine residues [12]. Ectopic expression of SIK1 in mouse livers reduces lipogenic gene expression and hepatic triglyceride accumulation [12]. This effect was reversed by co-expression of a

89 phosphorylation-deficient Srebp1-c mutant [17]. A previous report has shown that
90 lipogenic genes, such as FAS and ACC, are up-regulated by SIK1 knockdown in
91 mouse liver, whereas overexpression of SIK1 reduces expression levels of SREBP-1c
92 target genes, suggesting that SIK1 could regulate lipogenic gene transcript [17].
93 SIK1-induced phosphorylation of SREBP-1c at Ser329 is thought to be critical for the
94 suppression of SREBP-1c transcription activity [17]. Our previous study
95 demonstrated that overexpression of SIK1 suppressed the expression of SREBP-1c
96 and its target genes in HepG2 cells cultured in a high glucose environment [18]. Thus,
97 modulation of SREBP-1c activity by SIK1 would provide an attractive means for the
98 regulation of hepatic lipogenesis. In the diabetic conditions, normal regulation of
99 gluconeogenesis and lipogenesis is disrupted; hence the SIK1/CRTC2 and
100 SIK1/SREBP-1c pathways may serve as therapeutic targets to modulate metabolic
101 disorders in diabetic patients with NAFLD.

102 To date, the role and mechanism of SIK1 in the liver of the HFD/STZ-induced
103 T2DM rat model remains completely unknown. Because the diabetic rat model treated
104 with HFD plus low-dose STZ replicates the natural history and metabolic
105 characteristics of human T2DM and develops most of the biochemical and
106 pathological symptoms [19-24] associated with T2DM in humans, the diabetic rat
107 model is particularly suitable for pharmaceutical research [25]. Thus, it is of interest
108 to define the effect of SIK1 on hepatic gluconeogenesis and lipogenesis of the
109 HFD/STZ-induced T2DM rat. In the present study, we generates a diabetic rat model
110 treated with HFD plus low-dose STZ and focuses on the role of SIK1 in the hepatic

gluconeogenic and lipogenic pathways and their effect on the resulting phenotype of lower fasting glucose levels and ameliorated fatty liver disease. Meanwhile, we use a recombinant SIK1-expressing adenovirus to obtain a high expression of SIK1 in vivo, and then assess its affect on diabetes in the HFD/STZ-induced T2DM rat model. To our knowledge, this is the first study to examine the effects of adenovirus-mediated SIK1 overexpression on hepatic glucose and lipid metabolism in the HFD/STZ-induced T2DM rats.

Materials and Methods

Recombinant adenovirus production

Ad-Sik1 and negative control adenovirus containing green fluorescent protein (Ad-GFP) were purchased from Gene Chem Co., Ltd. (Shanghai, China). Ad-Sik1 and Ad-GFP were obtained with a titre of 1×10^{11} plaque forming units (PFU) /ml. The recombinant adenovirus was stored at –80°C until use. Construction of both vectors was described in S1 Appendix. Sik1-overexpressing rats were established by an injection of Ad-Sik1 or Ad-GFP at an optimized dose of 5×10^{9} PFU in 50μl (diluted with physiological saline) via tail vein once a week for 8 weeks according to the manufacturer's protocols. Meanwhile, the rats of the control and model groups received physiological saline at the same dosage by tail vein injection.

Animal treatments

Thirty male wistar rats, three to four-weeks-old, weighing approximately 70-100 g, were supplied by BEI JING HFK BIOSCIENCE CO., LTD (Beijing, China). The protocol for using animals was approved by the research Ethics Committee of Tongji

Medical College, Huazhong University of Science and Technology (Protocol Number: 822). All animals were housed with two rats per cage in an air-conditioned room (22°C ± 3°C, 50%-60% relative humidity) with a 12:12-hour light-dark cycle and were initially fed normal chow and allowed to adapt to their environment for 1 week. After acclimatization, all rats were randomly assigned to 2 groups. The control rats were fed ad libitum with a normal diet and the other rats were fed ad libitum with a HFD to induce diabetes [26]. Four weeks later, rats on HFD were injected with 36 mg/kg STZ (dissolved in citrate buffer, pH 4.5) intraperitoneally. Meanwhile, the control rats were injected with the same volume of citrate buffer. Diabetes was defined by fasting serum glucose >11.1 mmol/L 72 h after STZ injection. The diabetic rats were randomly divided into three groups: diabetes mellitus (DM) group (n=6), Ad-Sik1 group (n=8), and Ad-GFP group (n=6). The Ad-Sik1 and Ad-GFP groups received an injection of Ad-Sik1 or Ad-GFP at an optimized dose of 5×10^9 PFU via tail vein once a week for 8 weeks. The DM and normal control groups were given an equal volume of normal saline. The normal chow (13.68%, 64.44%, and 21.88% of calories derived, respectively, from fat, carbohydrate, and protein) was provided by the Laboratory Animal Center, Huazhong University of Science and Technology (Wuhan, China).The high fat diet (rodent diet with 45% kcal fat) was purchased from WANQIANJIAXING BIOTECHNOLOGY CO., LTD (Wuhan, China). Food intake, water intake and blood glucose were monitored periodically. After an 8-week treatment, the rats were weighed and sacrificed. Fasting blood was collected from the ventral aorta and serum was separated for biochemical analysis. The liver was

removed and weighed. Part of the liver was fixed in 4% paraformaldehyde and embedded in paraffin for hematoxylin and eosin (HE) staining and immunohistochemical analysis. The rest of the liver was washed with normal saline and stored at -80°C for RT-PCR and Western blot.

Reagents

STZ was purchased from Sigma (SaintLouis, Missouri, USA). RNAiso Plus was purchased from TaKaRa (Dalian, China). SIK1 antibody was purchased from Novus Biologicals, LLC (Cat #: 82417, Littleton, USA). SREBP-1c antibody, G6Pase and CRTC2 (S171) antibody were purchased from Abcam (Cat #: ab28481, Cat #: ab83690 and Cat #: ab203187, Cambrige, UK). CRTC2 antibody, SIK1 (S577) antibody, SIK1 (T182) antibody, FAS antibody and ACC antibody were purchased from Proteintech Group, Inc. (Cat #:12497-1-AP, Cat #: S4530-2, Cat #: S4529-2, Cat #:10624-2-AP and Cat #:21923-1-AP, Rosemont, USA). PEPCK antibody and β-actin antibody were purchased from Cell Signaling Technology, Inc. (Cat #: 12940 and Cat #: 4967, Danvers, Massachusetts, USA). Goldview DNA dye and DNA Marker I were purchased from TIANGEN BIOTECH (BEIJING) CO., LTD. Horseradish peroxidase-conjugated goat anti-rabbit IgG was purchased from Bioworld Technology, Inc. (Minnesota, USA) as secondary antibody.

Biochemical assay

Serum glucose was measured using enzymatic glucose-oxidase kits (Ruiyuan Biotechnology Co., Ltd, Ningbo, China), TG and total cholesterol (TC) were determined using enzymatic couple colorimetric kits (Huachen Biochemical Co., Ltd,

177 Shanghai, China).

178 Histological Analysis

179 Liver tissues were fixed in 4% paraformaldehyde for 24 h, embedded in paraffin,
180 sectioned into 4 μm sections (Leica, Wetzlar, Germany), and stained with HE for
181 microscopic assessment (Olympus, Tokyo, Japan). The liver cryosections were
182 prepared for oil red O staining.

183 Immunohistochemistry analysis

184 The liver tissues were fixed with 4% paraformaldehyde for paraffin embedding.
185 The paraffin-embedded sections were subjected to immunohistochemical staining for
186 SIK1, CRTC2, PEPCK, G6pase, SREBP-1c, FAS and ACC in the liver. The tissue
187 sections were incubated with rabbit anti primary antibody (1:100). After washing with
188 PBST, the sections were incubated with secondary antibody, and the
189 diaminobenzidine method was used. Next, the SIK1, CRTC2, PEPCK, G6pase,
190 SREBP-1c, FAS, ACC and Insulin protein expressions were observed under an
191 optical microscope. All the sections were examined by light microscope. Optical
192 density (OD) was identified as expression intensity of positive staining in the liver
193 tissues, which was semiquantitatively analysed with Image-Pro Plus 6.0 software
194 (Media Cybernetics, Inc., USA).

195 RT-PCR

196 Total RNA samples were isolated from the rat liver using RNAiso Plus (D9109;
197 TaKaRa, Dalian,China). RNA samples were converted to cDNA using a RevertAid
198 First Strand cDNA Synthesis Kit (Thermo Fisher Scientific, USA) according to the

199 manufacturer's instructions. Primers were designed using the nucleotide sequence and
200 synthesized by Sangon Biotechnology Co., Ltd. (Shanghai, China). Semi-quantitative
201 PCR conditions were 95°C for 2 minutes, 94°C for 30 seconds, followed by 35 cycles
202 at 55°C for 30 seconds, 72°C for 30 seconds, and 72°C for 2 minutes. PCR products
203 were separated by 1.5% agarose gel electrophoresis and visualised under ultraviolet
204 light using a JS-680B Bio-Imaging System camera (PEIQING Technology Limited,
205 Shanghai, China). Relative band intensities of each sample were calculated after being
206 normalized to the band intensity of β-actin. The sequences of the primers used in this
207 study are listed in S1 Table.

208 # Western blot

209 SIK1, SIK1 (S577), SIK1 (T182), CRTC2, CRTC2 (S171), PEPCK, G6pase,
210 SREBP-1c, FAS and ACC protein expression were determined by Western blotting,
211 which was performed according to standard procedures. The protein concentration in
212 tissue lysates was measured with a BCA protein assay kit (Boster, Wuhan, China)
213 according to the manufacturer's instructions. Protein lysates extracted from the rat
214 liver tissue were electrophoresed using 8-12% sodium dodecyl sulphate-
215 polyacrylamide gel electrophoresis (SDS-PAGE) for separation. Then, samples were
216 transferred onto a nitrocellulose membrane. The membrane was next incubated in 5%
217 milk in a mixture of Tris-buffered saline and Tween 20 (TBST) for 1 h at room
218 temperature to block the membrane. The proteins were incubated with the primary
219 antibody overnight at 4°C (SIK1, 1:1000; SIK1 (S577), 1:2000; SIK1 (T182), 1:2000;
220 CRTC2, 1:500; CRTC2 (S171), 1:500; PEPCK, 1:1000; G6pase, 1:800;SREBP-1c,

1:500; FAS, 1:500; ACC, 1:500; β-actin, 1:1000). After washing the membrane 5 times in TBST, the membrane was incubated with secondary antibody for 30 min at room temperature. Finally, the protein was detected with electrochemiluminescence (ECL) Western blotting reagents. The optical density (OD) of protein bands was quantified using Image J 1.48 software (National Institutes of Health, USA). The results are expressed as the ratio between the OD value of a target band to the OD value of β-actin.

Statistical analysis

All data are analysed by one-way ANOVA or two-way ANOVA using GraphPad Prism 5.0 software (GraphPad Software, San Diego, CA, USA), and the results are presented as the mean ± SD. $P<0.05$ was considered statistically significant. In the figures and tables, *P< 0.05; **P< 0.01; ***P< 0.001. ns, not significant.

Results

Effects on body weight, liver weight, FBG, TG and TC

Figure 1. Effects on body weight, liver weight, FBG, TG and TC in HFD/STZ-induced diabetic rats. (A) Body weight; (B) Liver weight; (C) Liver index; (D) Serum glucose levels ; (E) Serum TG levels ; (F) Serum TC levels . The results are expressed as the mean ±SD. Significant differences are indicated as *P<0.05, **P<0.01, *** P<0.001. ns, not significant.

The HFD/STZ-induced diabetic rats showed classic diabetic symptoms of polyuria, polydipsia and weight loss. These symptoms are related to the presence of hyperglycaemia (blood glucose level fluctuation from 20.09 to 30.61 mmol/L).

Neither the Ad-SIK1 group nor the Ad-GFP group showed significant differences in blood glucose or body weight. As shown in Table 1, serum glucose, TG and TC were significantly higher in the DM group compared to the control group. Intriguingly, serum TG was remarkably decreased ($P<0.05$), but serum TC slightly reduced in the Ad-SIK1 group compared to the DM group. Although Ad-SIK1 administration attenuated the HFD/STZ-induced increase in the serum TC level, no significant difference was observed.

Histological examination of liver

Fig 2. Effects on histology of liver of HFD/STZ-induced diabetic rats. (A) Liver tissue sections were stained with HE (×200); (B) oil red O to observe liver lipid content. Scale bar is 50 μm.

The typical HE and oil red O staining results obtained upon histological examination are shown in Fig 1. In consonance with the biochemical data, the staining of liver tissues with HE and oil red O revealed an accumulation of lipid droplets in the liver of the DM group, whereas lipid droplets were rare in the liver of the Ad-SIK1 group. Thus, Ad-SIK1 treatment significantly reduced fat deposition compared with the DM group, indicating that Ad-SIK1 administration could markedly improve steatosis. Therefore, these results confirmed the protective effect of SIK1 overexpression against histological changes in the liver of HFD/STZ-induced diabetic rats.

Immunohistochemical staining of genes related to hepatic glucose and lipid metabolism.

Fig.3 Effects on immunohistochemical staining of SIK1, CRTC2, PEPCK, G6pase, SREBP-1c, FAS and ACC in liver. (A) immunohistochemical staining of **SIK1, CRTC2, PEPCK and G6pase; (B)** immunohistochemical staining of **SREBP-1c, FAS and ACC.** Immunohistochemical staining images are 200 times larger under light microscopy Data are presented as the mean ± SD. Significant differences are indicated as * $p<0.05$, ** $p<0.01$, *** $p<0.001$. ns, not significant. Scale bar is 50 μm.

Fig 3 illustrates the immunohistochemical photomicrographs of SIK1, CRTC2, PEPCK, G6pase, SREBP-1c, FAS and ACC in the liver of rats. In the DM and Ad-GFP groups, SIK1-positive staining was much weaker than that in the Ad-SIK1 ($p<0.001$). Notably, SIK1 overexpression significantly increased the reduced SIK1-positive staining in the liver of diabetic rats. In contrast, CRTC2, PEPCK, G6pase, SREBP-1c, FAS and ACC stainings were much stronger in the DM and Ad-GFP groups than those in the Ad-SIK1 group ($p<0.001$). Obviously, Ad-SIK1 treatment inhibited this enhanced positive staining. In addition, we also verified that SIK1 overexpression inhibited CRTC2 nuclear translocation in the liver tissues *via* immunohistochemical staining. The nuclear expression of CRTC2 protein was obviously increased in the DM and Ad-GFP groups compared to the normal control group; however, the treatment with Ad-SIK1 inhibited the nuclear translocation of the CRTC2 protein.

SIK1 overexpression results in the inhibition of the hepatic gluconeogenic program in HFD/STZ-induced diabetic rats.

Fig 4. Effects on mRNA and protein expression of genes related to glucose metabolism in diabetic rats. (A) Protein levels of SIK1, CRTC2, PEPCK and G6pase in liver; (B) mRNA (relative fold change) levels of SIK1, CRTC2, PEPCK and G6pase in liver. Fold expression levels were measured relative to the expression of β-actin (internal control). Data are presented as the mean ± SD. Significant differences are indicated as * $p<0.05$, ** $p<0.01$, *** $p<0.001$. ns, not significant. n=6 in the control group; n=5 in the DM group; n=6 in the Ad-SIK1 group.

To determine whether SIK1 overexpression ameliorates hyperglycaemia by decreasing endogenous glucose production in the liver, we measured the mRNA and protein of SIK1, CRTC2, PEPCK and G6pase in the liver. RT-PCR analysis showed that SIK1 was significantly elevated in the Ad-SIK1 group compared to the DM group, while CRTC2, PEPCK and G6pase were significantly reduced, indicating an inhibitory effect of SIK1 in liver glucogenesis (Fig 3B). Indeed, the Western blot results showed that SIK1 was significantly decreased in the DM group compared to the control group, whereas CRTC2, PEPCK and G6pase were significantly elevated in the DM group. SIK1 overexpression significantly increased the protein level of SIK1, but decreased the protein levels of CRTC2, PEPCK and G6pase in liver compared with the DM group (Fig 3A). Meanwhile, the phosphorylation level of SIK1 at Ser577 was drastically reduced, whereas the level of pT182 SIK1 and pS171 CRTC2 was significantly increased in the Ad-SIK1 group compared with the DM and Ad-GFP groups. These results suggest that SIK1 could inhibit the hepatic gluconeogenic program in HFD/STZ-induced diabetic rats by regulating the SIK1/CRTC2 signalling

pathway.

SIK1 inhibits the hepatic lipogenic program in HFD/STZ-induced diabetic rats.

Fig 5. Effects on mRNA and protein expression of genes related to lipid metabolism in diabetic rats. (A) Protein levels of SREBP-1c, FAS and ACC in liver; (B) mRNA (relative fold change) levels of SREBP-1c, FAS and ACC in liver. Fold expression levels were measured relative to the expression of β-actin (internal control). Data are presented as the mean ± SD. Significant differences are indicated as * $p<0.05$, ** $p<0.01$, *** $p<0.001$. ns, not significant. n=6 in the control group; n=5 in the DM group; n=6 in the Ad-SIK1 group.

To investigate the underlying molecular mechanism of the hypolipidaemic effect of SIK1 overexpression on the diabetic rats, we measured the mRNA and protein of SREBP-1c, FAS and ACC in the liver. Notably, the mRNA expression of SREBP-1c, FAS and ACC in the liver of the DM group increased significantly compared to the control group (Fig 4B). However, Ad-SIK1 treatment significantly reduced the mRNA expression of SREBP-1c, FAS and ACC in the liver compared with the DM group, suggesting the mitigative role of SIK1 on fatty liver. Meanwhile, Western blot analysis revealed that SREBP-1c, FAS and ACC were markedly downregulated in the Ad-SIK1 group compared with the DM group (Fig 4A). Taken together, these findings indicate that the relieving effect of SIK1 overexpression on fatty liver was associated with a significant reduction in the expression of lipogenetic genes such as SREBP-1c, FAS and ACC.

Discussion

Since the discovery of the SIK family, the roles of SIK isoforms (SIK1/2/3) in glucose and lipid metabolism have been extensively investigated [6-9, 12, 14, 17, 18]. However, the biological function of SIK1 remains poorly understood in HFD/STZ-induced T2DM rats. In this study, we found that the expression of hepatic SIK1 was markedly decreased in the HFD/STZ-induced T2DM rat model and that administration of Ad-SIK1 lowered fasting blood glucose and ameliorated fatty liver disease, suggesting that a reduction of SIK1 may contribute to the glucose and lipid metabolism disorder in diabetes. Metformin, a widely used hypoglycemic drug, which attenuated hyperglycaemia and NAFLD in HFD/STZ-induced diabetic rats [27], increased SIK1 expression levels in HepG2 cells cultured in high glucose conditions [18]. These findings indicate that SIK1 may be associated with the pathogenesis of T2DM and NAFLD.

This study established a model of T2DM rats treated with HFD plus low-dose STZ. The HFD/STZ-induced diabetic rats exhibited classic diabetic symptoms of polyuria, polydipsia and weight loss. The T2DM rats also showed high blood glucose, high TG and TC than normal control rats, which was consistent with previous report [26]. We further determined the effect of Ad-SIK1 on hepatic glucose metabolism in HFD/STZ-induced diabetic rats. Although the function of SIK1 in the HFD/STZ-induced diabetic rat model has not been reported, but RNAi-based knockdown strategies and genetic diabetic mouse models have revealed its role in the regulation of glucose metabolism. First, overexpression of SIK1 reduced fasting blood

353 glucose and gluconeogenic gene expression in db/db mice, while Ad-SIK1 RNAi
354 promoted them [9]. Second, SIK1 activity was reduced in the livers of db/db diabetic
355 mice[12]. In the present study, the administration of Ad-SIK1 resulted in amelioration
356 of hyperglycaemia in HFD/STZ-induced diabetic rats, suggesting that exogenous
357 SIK1 might have a protective effect on T2DM. This is obviously the first report that
358 suggests the potential of adenovirus-mediated SIK1 gene transfer in the management
359 of hyperglycaemia in the HFD/STZ-induced T2DM rat model. More importantly, we
360 for the first time demonstrated that SIK1 mRNA and protein expression were
361 significantly reduced in the livers of HFD/STZ-induced diabetic rats, which was
362 consistent with our previous in vitro studies [8, 18], suggesting that the expression of
363 SIK1 is inhibited in diabetic states.

364 Phosphorylation at Thr182 by LKB1 is essential for switching on the SIK1
365 kinase activity [7, 28]. The Thr182 of SIK1 is phosphorylated by LKB1, resulting in
366 conversion from inactive SIK1 to the active form [6]. Consistent with previous in
367 vitro observations [8, 18], this in vivo study indicated that the level of Thr-182
368 phosphorylation, as well as the expression of SIK1 mRNA and protein, was
369 downregulated in the livers of HFD/STZ-induced diabetic rats, suggesting that the
370 SIK1 kinase activity may be suppressed in diabetic states. As expected, Ad-SIK1
371 treatment significantly elevated the level of pT182 SIK1 compared to the DM group.
372 In addition, the intracellular distribution of SIK1 is closely associated with its
373 functional activity. Ser-577 is a determinant of the intracellular distribution of SIK1.
374 Moreover, inactive SIK1 as well as CREB-repressing active SIK1 are present as

Ser577-dephosphorylated forms and are localized in the nucleus [3, 6, 8]. Phosphorylation of SIK1 at Ser577, which causes the nucleus export of SIK1, leads to a reduction of the transcriptional modulating activity of SIK1 [6]. On the basis of the ability of Ser 577 phosphorylation to decrease the transcriptional modulating activity of SIK1, we reasoned that phosphorylation level of Ser577 indicated the ability of SIK1 to suppress CREB. Thus, we examined the phosphorylation level of SIK1 at Ser577 in the livers of HFD/STZ-induced diabetic rats. In vivo, in the DM and Ad-GFP groups, the phosphorylation of SIK1 at Ser577 was elevated, whereas the expression of SIK1 was reduced, which were reversed by Ad-SIK1 administration, suggesting the possibility that SIK1 acts as a modulator of CREB-dependent transcription in the livers of HFD/STZ-induced diabetic rats.

The remarkable feature of T2DM is elevated fasting blood glucose. Dysregulated gluconeogenesis contributes to hyperglycaemia in diabetic rodents and humans [29, 30]. SIK1 was shown to inhibit CREB activity by phosphorylating CREB-specific coactivators, CRTC2, at Ser171 to suppress hepatic gluconeogenesis [9, 10]. Serine 171 is the primary phosphorylation site that mediates CRTC2 activity [9]. To confirm the importance of Ser 171 for inhibition of the gluconeogenic programme by SIK1, we evaluated the expression of hepatic SIK1, CRTC2 and pS171 CRTC2 in diabetic rats. Our results showed that the mRNA and protein expression of CRTC2 in the DM and Ad-GFP groups was significantly elevated, whereas pS171 CRTC2 was downregulated compared to the control group. Moreover, relative to control Ad-GFP diabetic rats, Ad-SIK1 administration decreased fasting blood glucose, increased

pS171 CRTC2 and reduced CRTC2 and gluconeogenic genes, such as PEPCK and G6Pase. The changes in expression of SIK1, CRTC2, PEPCK and G6Pase were also confirmed by immunohistochemistry analysis. Interestingly, the CRTC2 nuclear accumulation observed in the Ad-SIK1 group was lower than that seen in the DM group, suggesting that Ad-SIK1 treatment might deter the translocation of CRTC2 into the cell nucleus, thus reducing the transcription of gluconeogenic genes and hepatic glucose output. Consequently, we observed lower blood glucose levels in the Ad-SIK1 group than in the DM group. Taken together, these findings suggest that recombinant SIK1 directly inhibited the hepatic gluconeogenic program in the HFD/STZ-induced diabetic rats by the SIK1/CRTC2 pathway.

Lipid metabolic disorder is one of the most common pathophysiological changes in T2DM. Liver plays a vital role in the regulation of systemic lipid metabolism. As a key regulator of hepatic lipogenesis, SREBP-1c was suggested to be involved in the development of NAFLD by contributing to the onset of fatty liver phenotypes [17]. SIK1 regulates hepatic lipogenesis by modulating SREBP-1c activity [17]. To evaluate the effect of adenovirus-mediated SIK1 overexpression on lipogenic gene expression in the livers of HFD/STZ-induced T2DM rats, we transduced diabetic rats with Ad-SIK1 adenovirus or Ad-GFP control viruses. In this study, the HFD/STZ-induced diabetic rats showed characteristics of NAFLD, including elevation of hepatic enzyme levels, significantly increased relative liver weights (liver index), hyperlipidaemia and histological changes such as steatosis and hepatocyte injury. In concert with the histological and immunohistochemistry analysis,

Ad-SIK1 administration reduced serum TC and TG levels, and decreases the elevated hepatic mRNA and protein levels of SREBP-1c, FAS and ACC caused by HFD/STZ-induced T2DM, suggesting that overexpression of SIK1 could suppress hepatic lipogenesis by downregulating SREBP-1c and its downstream gene expression. This effect was consistent with previous reports [12, 17].

In summary, the present study demonstrates that SIK1 mRNA and protein expression are significantly reduced in the livers of HFD/STZ-induced diabetic rats. Overexpression of SIK1 ameliorates hyperglycaemia and fatty liver by suppressing hepatic gluconeogenesis and lipogenesis in HFD/STZ-induced T2DM rats. This protective effect of SIK1 may be derived from its interference with the SIK1/CRTC2 and SIK1/SREBP-1c pathways. Up-regulating hepatic SIK1 expression may represent an attractive means for the treatment of T2DM and NAFLD. Figure 6 illustrates the possible mechanisms of SIK1 in attenuating T2DM with NAFLD.

Figure 6. Proposed mechanisms of the hypoglycemic and hypolipidemic effect of SIK1. Schematic representation of the role of SIK1 in amelioration of T2DM with NAFLD. Overexpression of SIK1 can contribute to preventing hyperglycemia and hepatic lipid accumulation through suppressing gluconeogenesis and lipogenesis with a decrease in the expressions of CRTC2, PEPCK, G6Pase, SREBP-1c, FAS and ACC in liver, thus reducing fasting blood glucose, serum TC, serum TG, hepatic steatosis and liver weight. SIK1, salt-induced kinase 1; CRTC2, CREB-regulated transcription co-activator 2; PEPCK, phosphoenolpyruvate carboxykinase; G6Pase, glucose-6-phosphatase; SREBP-1c, sterol regulatory element binding-protein-1c;

441 ACC, acetyl-CoA carboxylase; FAS, fatty acid synthase; TC, total cholesterol; TG
442 triglycerides.
443

444 Supporting Information

445 **S1 Appendix.** Method of construction of recombinant adenovirus vectors.

446 **S1 Table.** List of primer sequences for RT-PCR.

447 **S2 Table.** Changes in body weight, liver weight, FBG, TG and TC.
448

449 **Author Contributions:** Conceptualization, XiuYing Wen; Data curation,
450 DaoFei Song and Chang Wang; Formal analysis, DaoFei Song and Lei Yin; Funding
451 acquisition, XiuYing Wen; Investigation, DaoFei Song; Methodology, XiuYing Wen;
452 Project administration, DaoFei Song; Supervision, XiuYing Wen; Validation, DaoFei
453 Song; Writing – original draft, DaoFei Song; Writing – review & editing, XiuYing
454 Wen.

455 **Conflict of interest:** The authors declare that there are no conflicts of
456 interest.
457

458 Abbreviations

459 ACC acetyl-CoA carboxylase
460 ACTH adrenocorticotropic hormone
461 Ad-GFP adenovirus-green fluorescent protein
462 Ad-SIK1 adenovirus-Salt induced kinase 1
463 AMPK AMP-activated protein kinase

CREB	cAMP response element binding protein
CRTC2	CREB-regulated transcription co-activator 2
DM	diabetes mellitus
FAS	fatty acid synthase
G6Pase	glucose-6-phosphatase
HFD	high-fat diet
LKB1	serine/threonine kinase 11
NAFLD	nonalcoholic fatty liver disease
OD	optical density
PGC-1α	peroxisome proliferator-activated receptor gamma coactivator 1-alpha
PKA	protein kinase A
PEPCK	phosphoenolpyruvate carboxykinase
PFU	plaque forming units
RT-PCR	reverse transcription-polymerase chain reaction
SIK1	Salt-induced kinase 1
STZ	streptozotocin
SREBP-1c	regulatory element binding-protein-1c
T2DM	type 2 diabetes mellitus
TC	total cholesterol
TG	triglycerides

References

1. Diagnosis and classification of diabetes mellitus. *Diabetes care* **2014,** 37 Suppl 1,

S81-90.

2. Phillips, C. A.; Molitch, M. E., The relationship between glucose control and the development and progression of diabetic nephropathy. *Current diabetes reports* **2002,** 2, (6), 523-9.

3. Takemori, H.; Katoh, Y.; Horike, N.; Doi, J.; Okamoto, M., ACTH-induced nucleocytoplasmic translocation of salt-inducible kinase. Implication in the protein kinase A-activated gene transcription in mouse adrenocortical tumor cells. *The Journal of biological chemistry* **2002,** 277, (44), 42334-43.

4. Quan, H. Y.; Yuan, H. D.; Jung, M. S.; Ko, S. K.; Park, Y. G.; Chung, S. H., Ginsenoside Re lowers blood glucose and lipid levels via activation of AMP-activated protein kinase in HepG2 cells and high-fat diet fed mice. *International journal of molecular medicine* **2012,** 29, (1), 73-80.

5. Steinberg, G. R.; Kemp, B. E., AMPK in Health and Disease. *Physiological reviews* **2009,** 89, (3), 1025-78.

6. Katoh, Y.; Takemori, H.; Lin, X. Z.; Tamura, M.; Muraoka, M.; Satoh, T.; Tsuchiya, Y.; Min, L.; Doi, J.; Miyauchi, A.; Witters, L. A.; Nakamura, H.; Okamoto, M., Silencing the constitutive active transcription factor CREB by the LKB1-SIK signaling cascade. *The FEBS journal* **2006,** 273, (12), 2730-48.

7. Hashimoto, Y. K.; Satoh, T.; Okamoto, M.; Takemori, H., Importance of autophosphorylation at Ser186 in the A-loop of salt inducible kinase 1 for its sustained kinase activity. *Journal of cellular biochemistry* **2008,** 104, (5), 1724-39.

8. Yu, J.; Hu, X.; Yang, Z.; Takemori, H.; Li, Y.; Zheng, H.; Hong, S.; Liao, Q.; Wen,

509 X., Salt-inducible kinase 1 is involved in high glucose-induced mesangial cell
510 proliferation mediated by the ALK5 signaling pathway. *International journal of*
511 *molecular medicine* **2013,** 32, (1), 151-7.
512 9. Koo, S. H.; Flechner, L.; Qi, L.; Zhang, X.; Screaton, R. A.; Jeffries, S.; Hedrick,
513 S.; Xu, W.; Boussouar, F.; Brindle, P.; Takemori, H.; Montminy, M., The CREB
514 coactivator TORC2 is a key regulator of fasting glucose metabolism. *Nature* **2005,**
515 437, (7062), 1109-11.
516 10. Lin, H. V.; Accili, D., Hormonal regulation of hepatic glucose production in
517 health and disease. *Cell metabolism* **2011,** 14, (1), 9-19.
518 11. Herzig, S.; Long, F.; Jhala, U. S.; Hedrick, S.; Quinn, R.; Bauer, A.; Rudolph,
519 D.; Schutz, G.; Yoon, C.; Puigserver, P.; Spiegelman, B.; Montminy, M., CREB
520 regulates hepatic gluconeogenesis through the coactivator PGC-1. *Nature* **2001,**
521 413, (6852), 179-83.
522 12. Berdeaux, R., *Metabolic regulation by salt inducible kinases*. 2011; Vol. 6,
523 p 231-241.
524 13. Doi, J.; Takemori, H.; Lin, X. Z.; Horike, N.; Katoh, Y.; Okamoto, M.,
525 Salt-inducible kinase represses cAMP-dependent protein kinase-mediated
526 activation of human cholesterol side chain cleavage cytochrome P450 promoter
527 through the CREB basic leucine zipper domain. *The Journal of biological*
528 *chemistry* **2002,** 277, (18), 15629-37.
529 14. Patel, K.; Foretz, M.; Marion, A.; Campbell, D. G.; Gourlay, R.; Boudaba, N.;
530 Tournier, E.; Titchenell, P.; Peggie, M.; Deak, M.; Wan, M.; Kaestner, K. H.;

Goransson, O.; Viollet, B.; Gray, N. S.; Birnbaum, M. J.; Sutherland, C.; Sakamoto, K., The LKB1-salt-inducible kinase pathway functions as a key gluconeogenic suppressor in the liver. *Nature communications* **2014,** 5, 4535.

15. Biddinger, S. B.; Kahn, C. R., From mice to men: insights into the insulin resistance syndromes. *Annual review of physiology* **2006,** 68, 123-58.

16. Bugianesi, E.; McCullough, A. J.; Marchesini, G., Insulin resistance: a metabolic pathway to chronic liver disease. *Hepatology (Baltimore, Md.)* **2005,** 42, (5), 987-1000.

17. Yoon, Y. S.; Seo, W. Y.; Lee, M. W.; Kim, S. T.; Koo, S. H., Salt-inducible kinase regulates hepatic lipogenesis by controlling SREBP-1c phosphorylation. *The Journal of biological chemistry* **2009,** 284, (16), 10446-52.

18. Zhang, Y.; Takemori, H.; Wang, C.; Fu, J.; Xu, M.; Xiong, L.; Li, N.; Wen, X., Role of salt inducible kinase 1 in high glucose-induced lipid accumulation in HepG2 cells and metformin intervention. *Life sciences* **2017,** 173, 107-115.

19. Srinivasan, K.; Viswanad, B.; Asrat, L.; Kaul, C. L.; Ramarao, P., Combination of high-fat diet-fed and low-dose streptozotocin-treated rat: a model for type 2 diabetes and pharmacological screening. *Pharmacological research* **2005,** 52, (4), 313-20.

20. Islam, M. S.; Choi, H., Nongenetic model of type 2 diabetes: a comparative study. *Pharmacology* **2007,** 79, (4), 243-9.

21. Breant, B.; Gesina, E.; Blondeau, B., Nutrition, glucocorticoids and pancreas development. *Hormone research* **2006,** 65 Suppl 3, 98-104.

553 22. Reed, M. J.; Meszaros, K.; Entes, L. J.; Claypool, M. D.; Pinkett, J. G.; Gadbois,
554 T. M.; Reaven, G. M., A new rat model of type 2 diabetes: the fat-fed,
555 streptozotocin-treated rat. *Metabolism: clinical and experimental* **2000,** 49, (11),
556 1390-4.
557 23. Masiello, P.; Broca, C.; Gross, R.; Roye, M.; Manteghetti, M.; Hillaire-Buys, D.;
558 Novelli, M.; Ribes, G., Experimental NIDDM: development of a new model in
559 adult rats administered streptozotocin and nicotinamide. *Diabetes* **1998,** 47, (2),
560 224-9.
561 24. Pascoe, W. S.; Storlien, L. H., Inducement by fat feeding of basal hyperglycemia
562 in rats with abnormal beta-cell function. Model for study of etiology and
563 pathogenesis of NIDDM. *Diabetes* **1990,** 39, (2), 226-33.
564 25. Islam, M.; Loots, D. T., Experimental rodent models of Type 2 Diabetes: A
565 Review. *Methods and Findings in Experimental and Clinical Pharmacology* **2009,**
566 31, 249.
567 26. Wen, X.; Zeng, Y.; Liu, L.; Zhang, H.; Xu, W.; Li, N.; Jia, X., Zhenqing recipe
568 alleviates diabetic nephropathy in experimental type 2 diabetic rats through
569 suppression of SREBP-1c. *Journal of ethnopharmacology* **2012,** 142, (1), 144-50.
570 27. Jiang, S. J.; Dong, H.; Li, J. B.; Xu, L. J.; Zou, X.; Wang, K. F.; Lu, F. E.; Yi, P.,
571 Berberine inhibits hepatic gluconeogenesis via the LKB1-AMPK-TORC2 signaling
572 pathway in streptozotocin-induced diabetic rats. *World journal of gastroenterology*
573 **2015,** 21, (25), 7777-85.
574 28. Lizcano, J. M.; Goransson, O.; Toth, R.; Deak, M.; Morrice, N. A.; Boudeau, J.;

575 Hawley, S. A.; Udd, L.; Makela, T. P.; Hardie, D. G.; Alessi, D. R., LKB1 is a
576 master kinase that activates 13 kinases of the AMPK subfamily, including
577 MARK/PAR-1. *The EMBO journal* **2004,** 23, (4), 833-43.
578 29. Magnusson, I.; Rothman, D. L.; Katz, L. D.; Shulman, R. G.; Shulman, G. I.,
579 Increased rate of gluconeogenesis in type II diabetes mellitus. A 13C nuclear
580 magnetic resonance study. *The Journal of clinical investigation* **1992,** 90, (4),
581 1323-7.
582 30. Yoon, J. C.; Puigserver, P.; Chen, G.; Donovan, J.; Wu, Z.; Rhee, J.; Adelmant,
583 G.; Stafford, J.; Kahn, C. R.; Granner, D. K.; Newgard, C. B.; Spiegelman, B. M.,
584 Control of hepatic gluconeogenesis through the transcriptional coactivator PGC-1.
585 *Nature* **2001,** 413, (6852), 131-8.
586
587

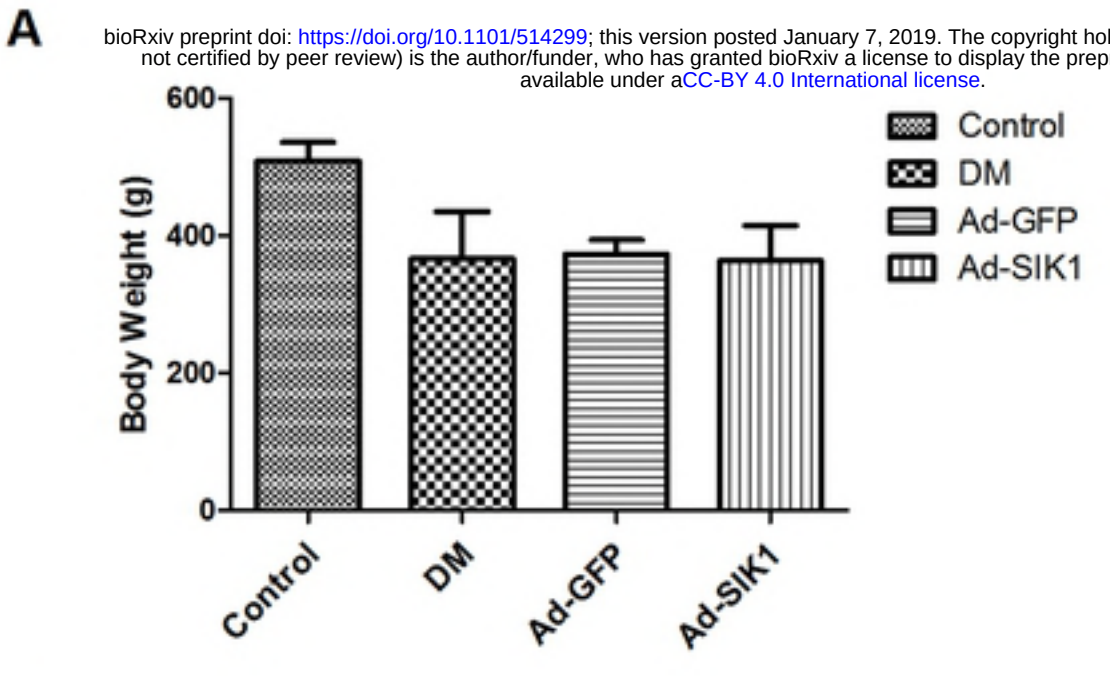

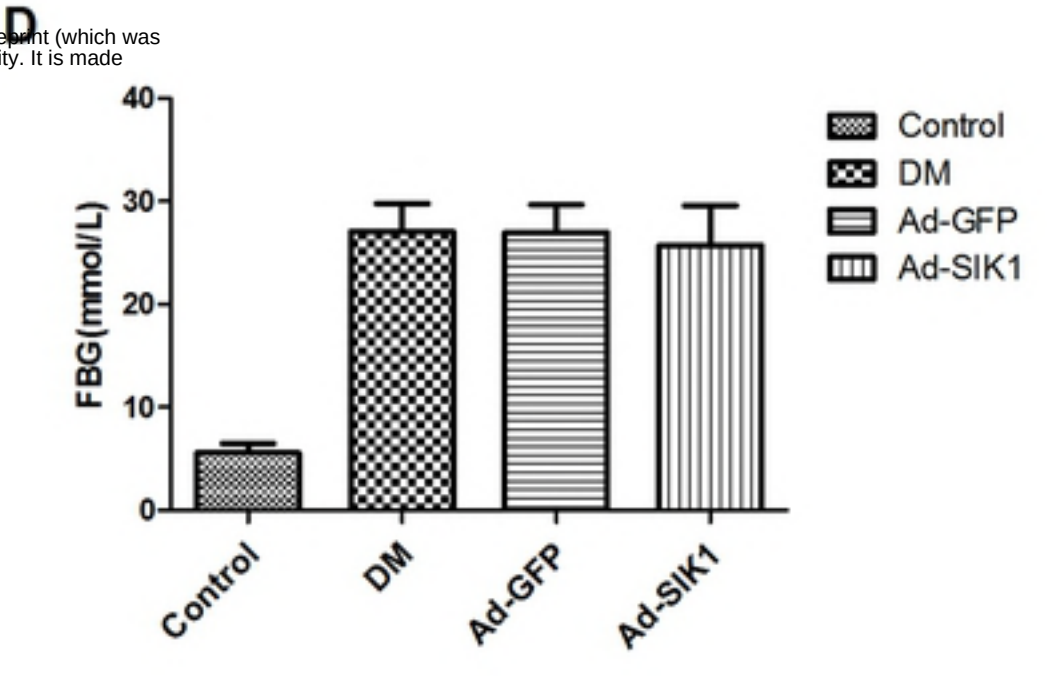

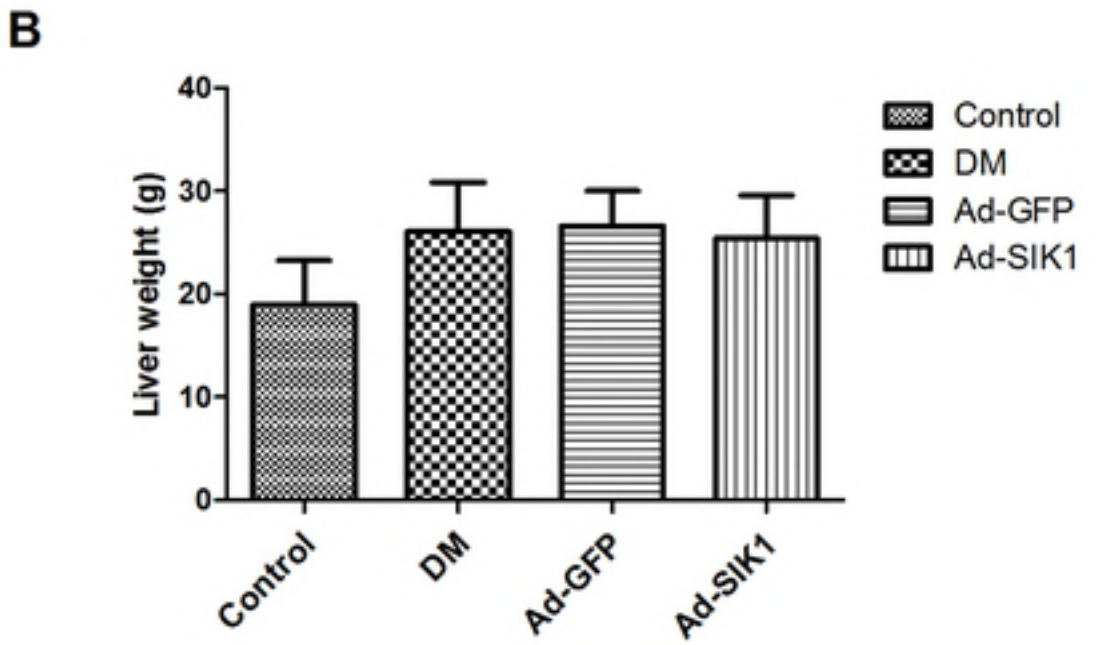

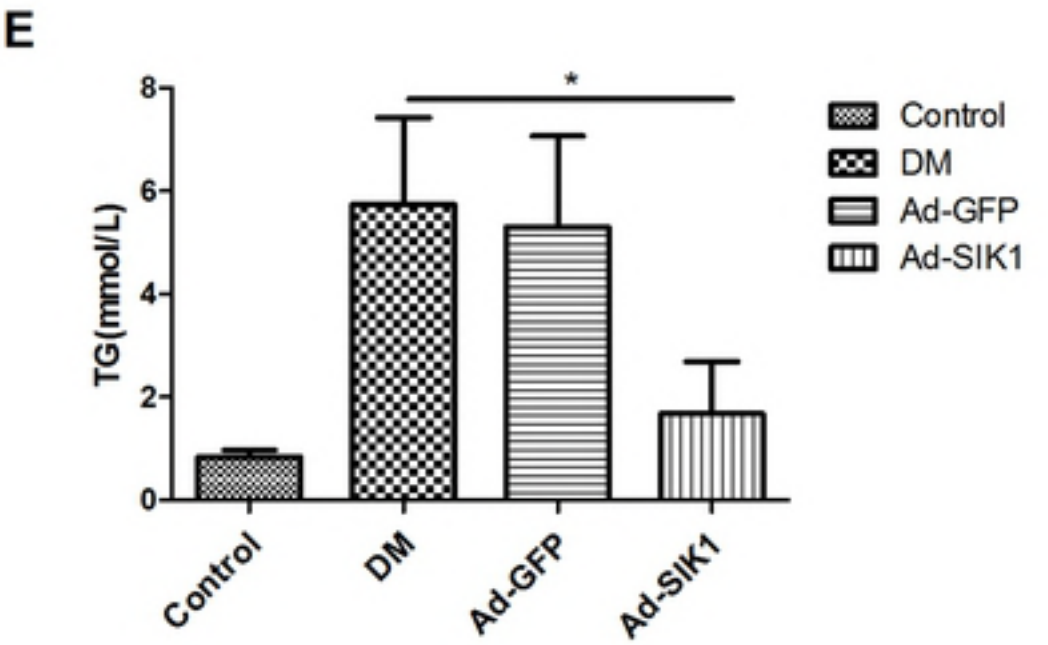

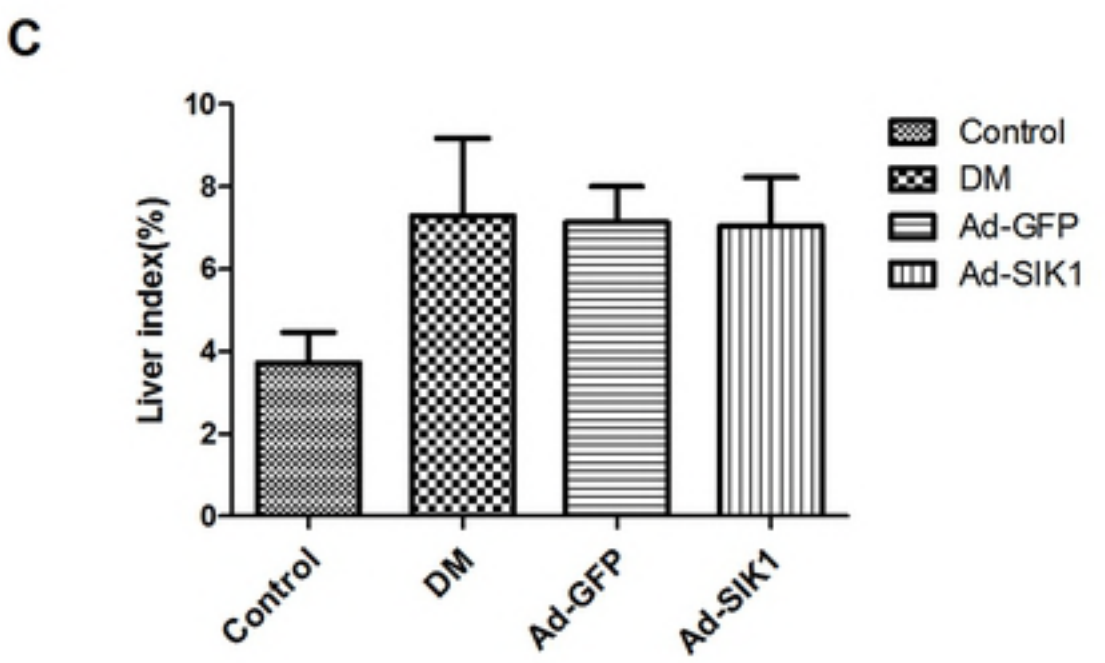

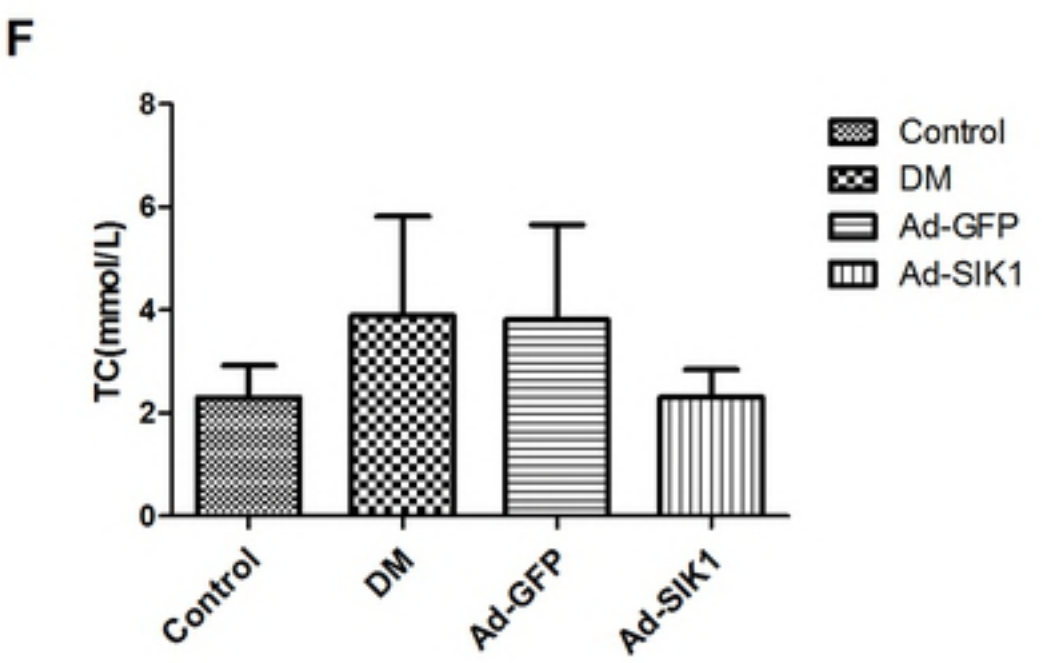

Figure1

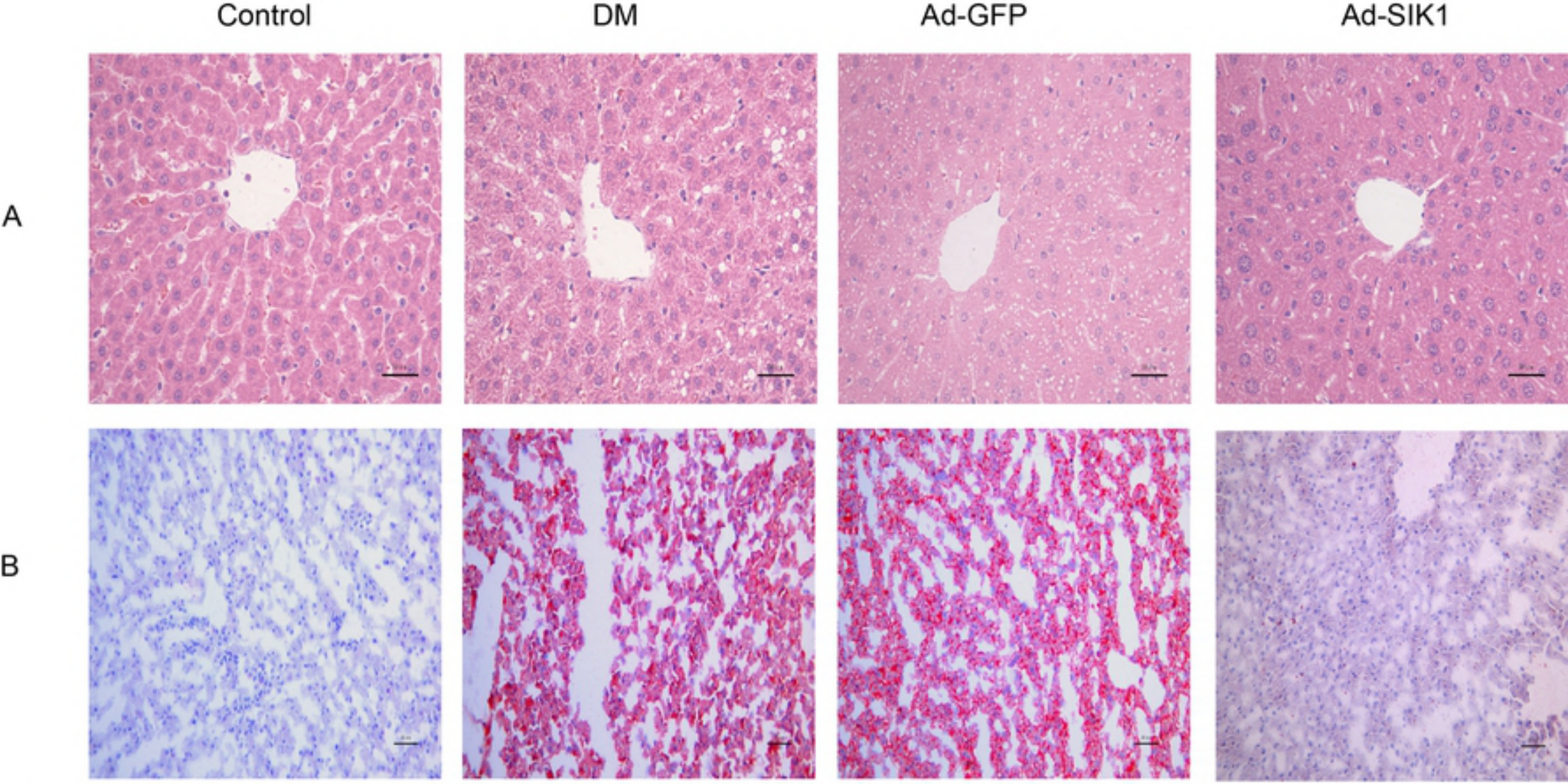

Figure2

A

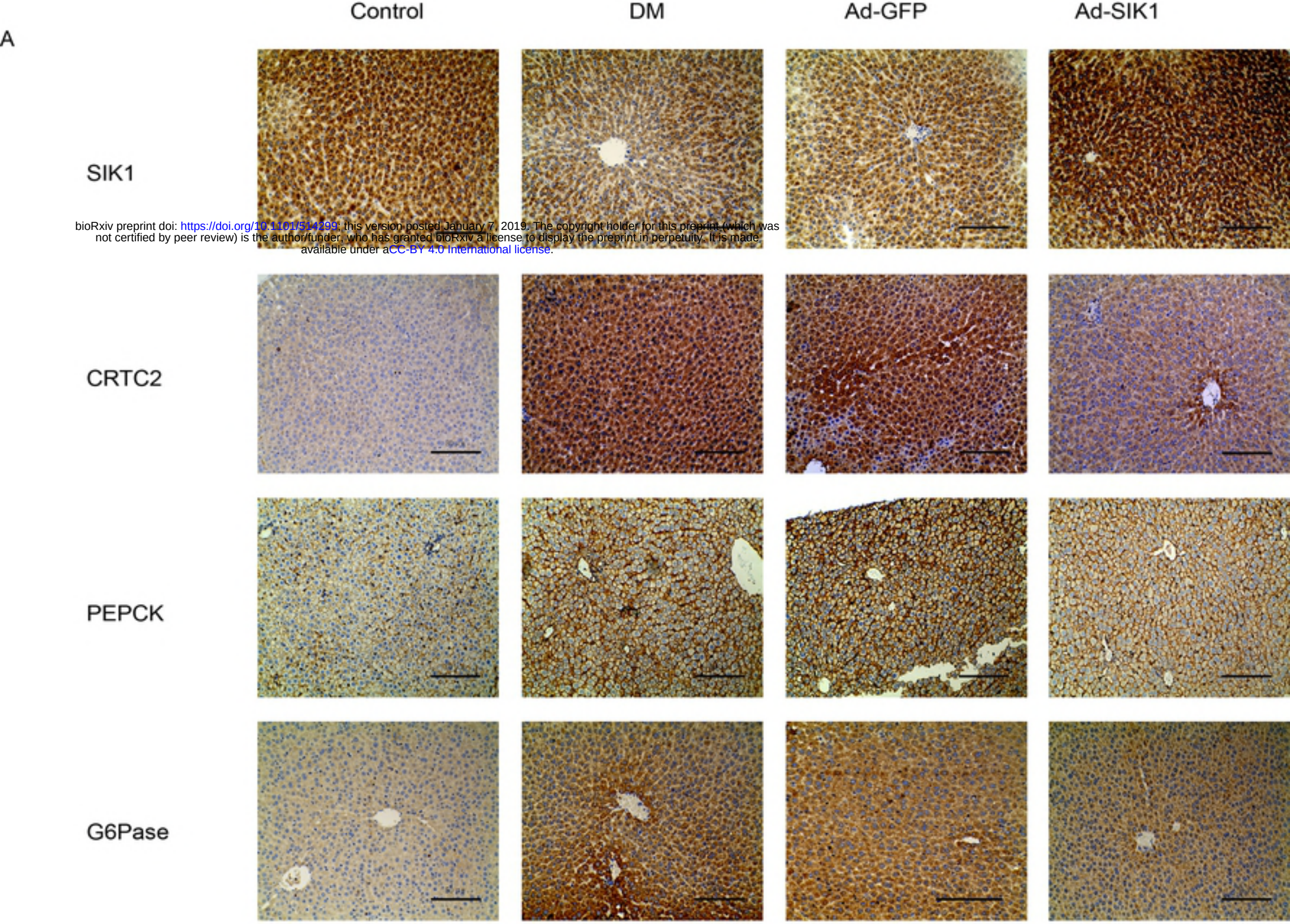

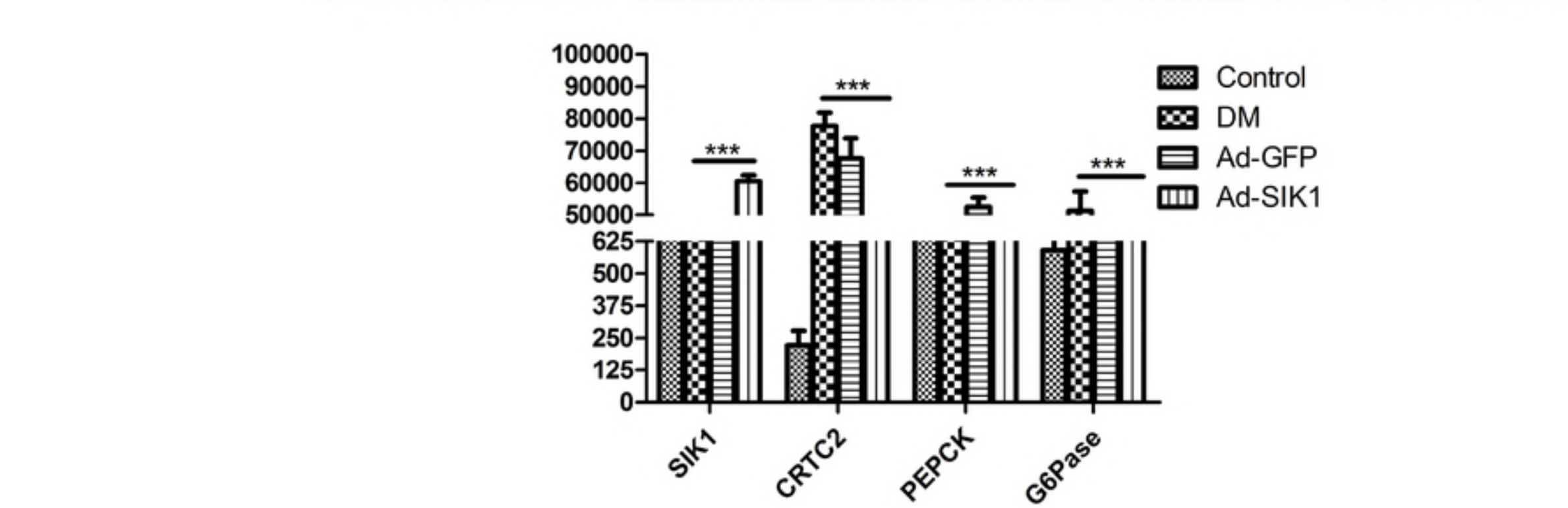

Figure3A

B

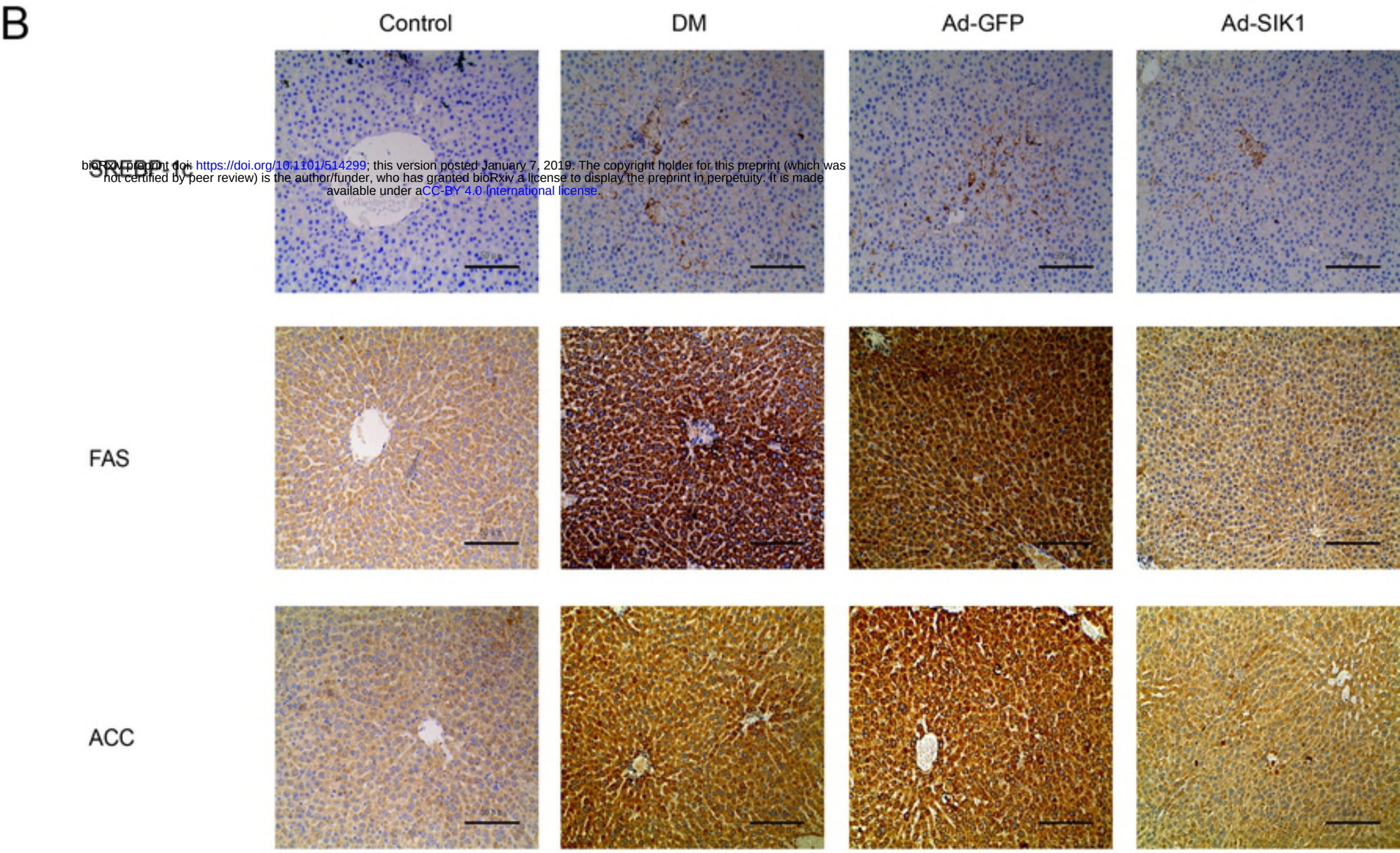

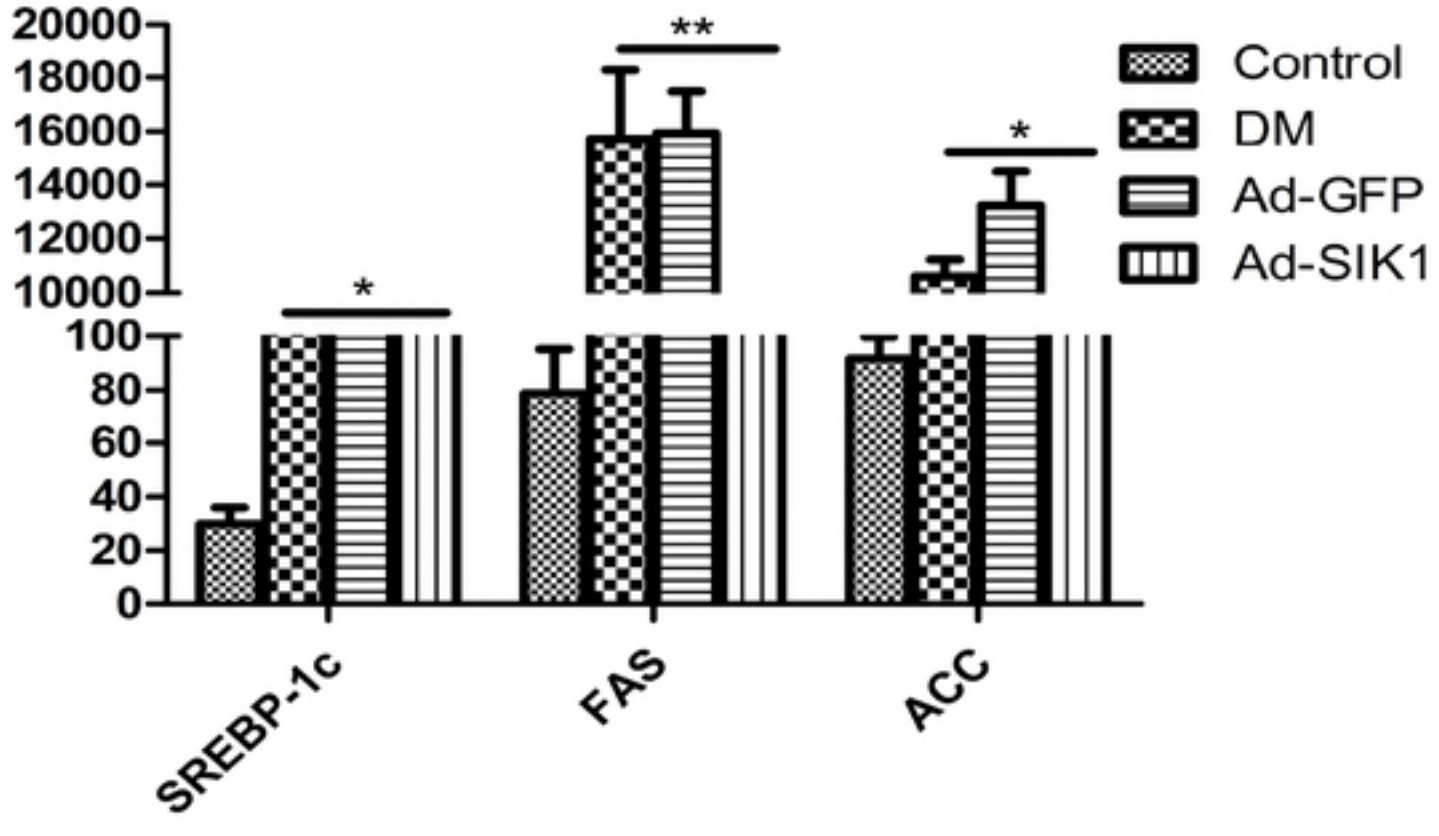

Figure3B

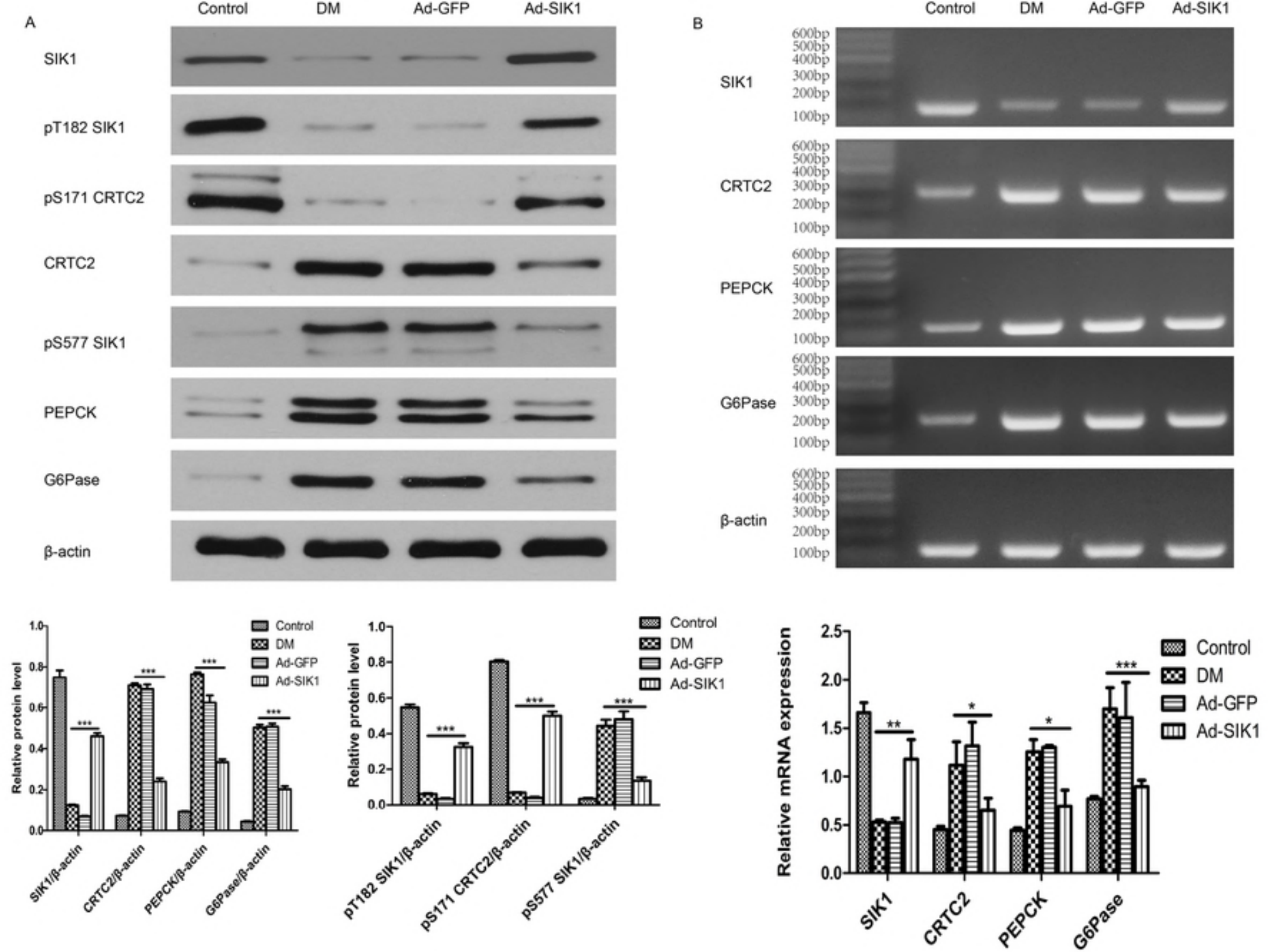
A
Control
DM
Ad-GFP
Ad-SIK1
SIK1
pT182 SIK1
pS171 CRTC2
CRTC2
pS577 SIK1
PEPCK
G6Pase
β-actin
B
Control
DM
Ad-GFP
Ad-SIK1
SIK1
CRTC2
PEPCK
G6Pase
β-actin
600bp
500bp
400bp
300bp
200bp
100bp
Relative protein level
SIK1/β-actin
CRTC2/β-actin
PEPCK/β-actin
G6Pase/β-actin
pT182 SIK1/β-actin
pS171 CRTC2/β-actin
pS577 SIK1/β-actin
Relative mRNA expression
***
**
*

Figure4

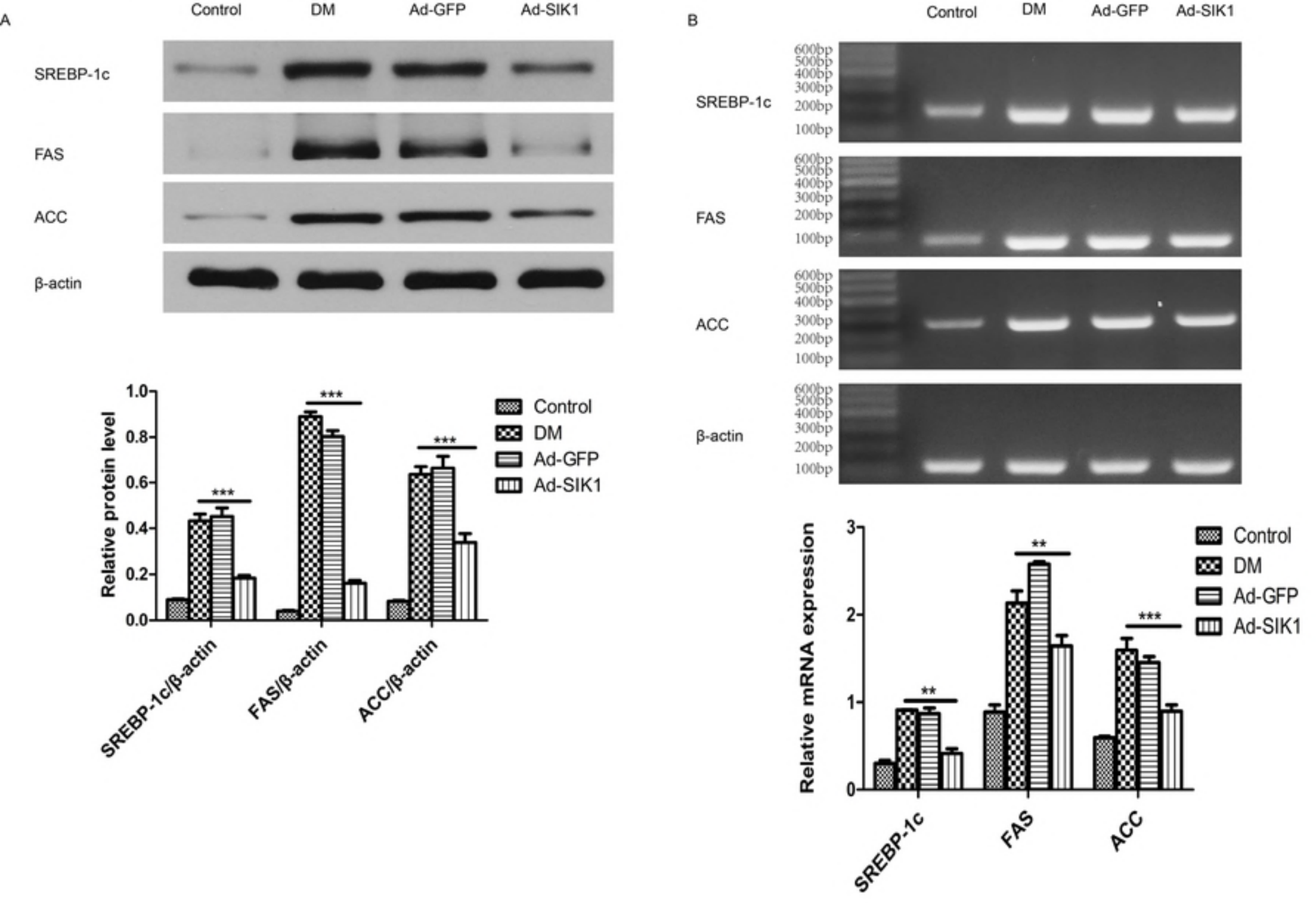
A
Control
DM
Ad-GFP
Ad-SIK1
SREBP-1c
FAS
ACC
β-actin
Relative protein level
1.0
0.8
0.6
0.4
0.2
0.0
***
***
***
Control
DM
Ad-GFP
Ad-SIK1
SREBP-1c/β-actin
FAS/β-actin
ACC/β-actin
B
Control
DM
Ad-GFP
Ad-SIK1
SREBP-1c
FAS
ACC
β-actin
600bp
500bp
400bp
300bp
200bp
100bp
Relative mRNA expression
3
2
1
0
**
**
***
Control
DM
Ad-GFP
Ad-SIK1
SREBP-1c
FAS
ACC

Figure5

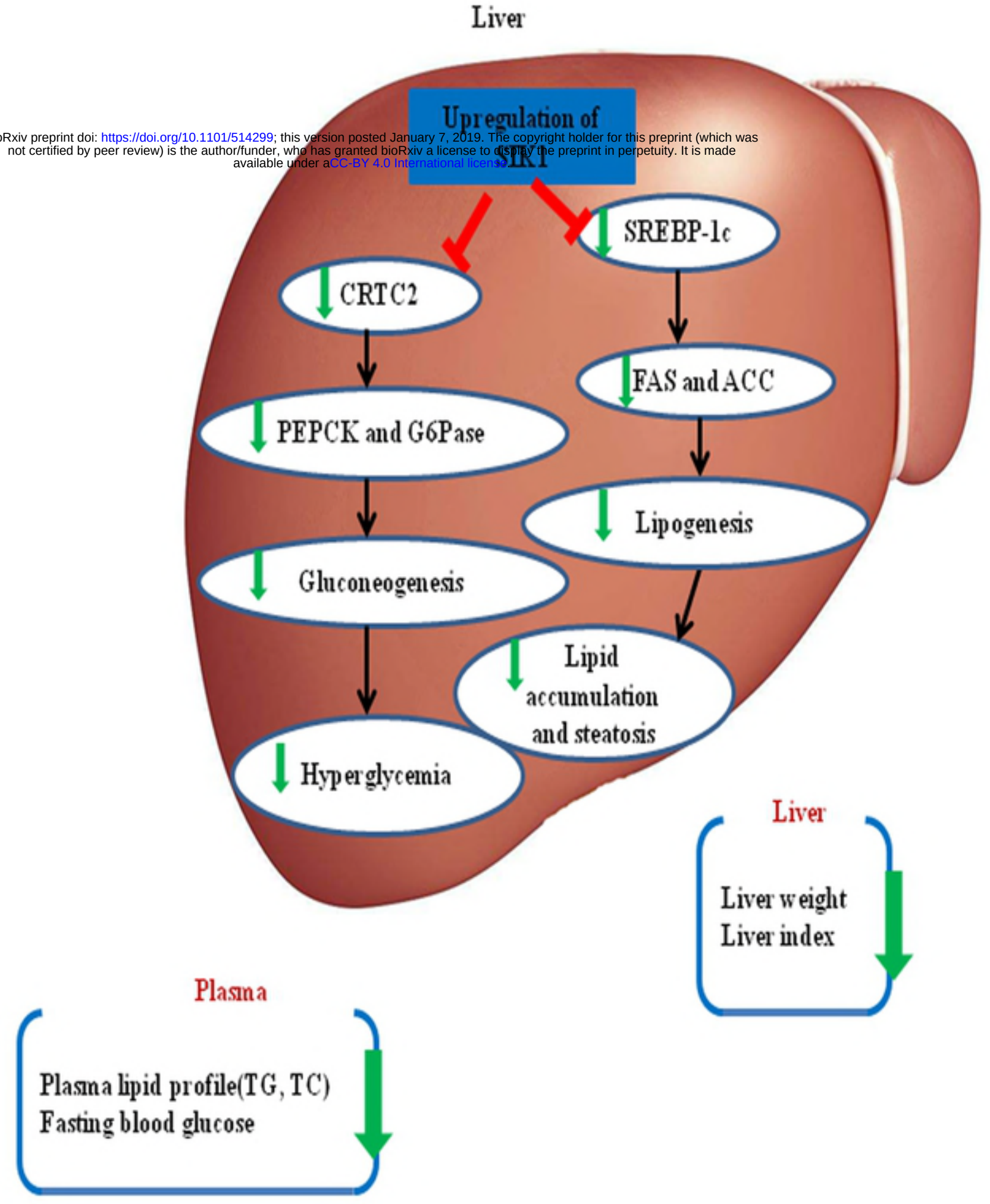

Figure6